Deuteron photodisintegration

Shuqian Ying, E. M. Henley, and G. A. Miller
Institute for Nuclear Theory, Department of Physics, FM-15, University of Washington, Seattle, Washington 98195
(Received 13 May 1988)

The photodisintegration of the deuteron is investigated with emphasis on the differential cross section $D(\gamma,p)n$ in the forward direction. However the angular distribution as well as the γ asymmetry are also given. The calculation takes relativistic, pion exchange, and $\Delta(1232)$ corrections into account. Nonlocal nucleon-nucleon interactions are treated in a manner in which gauge invariance is respected. The differences between various approximations beyond the Siegert limit are discussed. The role of the D-state probability of the deuteron in the forward direction is studied and the difference of two gauges before and after the inclusion of various corrections are presented. Finally a comparison with experiment is carried out.

I. INTRODUCTION

There is a well-known discrepancy between the theoretical forward differential cross section for the photodisintegration of the deuteron $D(\gamma,p)n$ calculated in the nonrelativistic impulse approximation (NRIA) and the experimental value.[1] Partovi wrote the general expression for the photodisintegration amplitude in the nonrelativistic impulse approximation for arbitrary multipoles of the radiation field.[2] However, for photon laboratory energies above 20 MeV, Partovi's prediction for the forward direction scattering cross section is 20–30 % larger than the experimental values.[1] Although the failure of the simple nonrelativistic impulse approximation in this energy region is not surprising, the magnitude of the discrepancy is startling. It signals the importance of corrections, such as (1) relativistic effects, (2) mesonic + $\Delta(1232)$ effects, and (3) short-range corrections. In addition, it is commonly stated[3–6] that the forward direction differential cross section of the photodisintegration of the deuteron is sensitive to the D-state probability of the deuteron. Since the theoretical forward differential cross section[6] still lies above the experimental value[1] for a detailed analysis and calculation with the Paris potential,[7] we have investigated the possibility of further reducing the theoretical cross section in the forward direction by using the one boson exchange coordinate-space (OBEPR) Bonn potential[8] which has a low D-state percentage (4.8%) but which was derived from a sound one boson exchange theoretical model, and gives reasonable fits to both bound state and scattering data.

Cambi, Mosconi, and Ricci[9] were the first ones to investigate relativistic corrections. They found that the application of the well-known spin-orbit and Darwin-Foldy[10] terms in the charge density significantly reduced the discrepancy between theory and experiment. These terms were generated through the Foldy-Wouthuysen (FW) transformation of the relativistic charge density operator. More recently a more thorough treatment of a relativistic correction has been carried out by Jaus and Woolcock.[11] It is based on a Blankenbecler-Sugar[12] reduction of the Bethe-Salpeter equation with the spinor reduction carried out to $O(m_N^{-2})$ for the charge and current densities. Similar work with different approaches have been done by other authors.[13] We use the results given by Jaus and Woolcock[11] in this paper.

The meson and Δ resonance corrections to the process $D(\gamma,p)n$ have been investigated by various authors.[6,13–15] The pion current correction has been universally used. Issues have been raised with respect to pion charge density; all center on the consistent treatment of the pion exchange for both the long distance NN and the electromagnetic interactions. The pseudoscalar (PS) and pseudovector (PV) couplings of a pion with a nucleon are equivalent to lowest order in the coupling, as can be shown by a FW type unitary transformation[16] (Dyson transformation). However, the equivalence is broken in the presence of an electromagnetic interaction.[17] Many studies have been gathering evidence in favor of PV coupling both for the NN interaction,[8] as well as for the electromagnetic interaction of the NN system with the radiation field.[18] The leading contribution from the 1π exchange terms to the NN potential (static term) are the same both for PS and PV coupling. However, the retardation parts are different. These differences can be compensated by a unitary transformation of the short-range part of the NN potential such that both the NN phase shifts and the deuteron properties fit the experimental values. Most of the phenomenological NN potentials do not distinguish between PS and PV coupling; the retardation is either dropped completely or only partially included. Even for the OBEPR (Ref. 8) Bonn potential the retardation part is dropped, although the full model in momentum space includes all of the retardation in PV coupling. Fortunately, this unsatisfactory situation can be circumvented perturbatively in a reasonable way by introducing an additional effective charge density.[11] However, a more satisfactory treatment would rely on a more realistic NN potential (with PV coupling and retardation effects taken into account). The $\Delta(1232)$ contribution also needs to be included for a complete description of the $D(\gamma,p)n$ reaction. It reduces the difference between theoretical and experimental values of the angular distribution and the γ asymmetry.[6,15]

For consistency, gauge invariance has to be respected. The nonlocality of the *NN* potential breaks gauge invariance and this needs to be restored in a reasonable way. As shown in Ref. 19 there is no unique way to write down a gauge invariant *NN* potential if one does not start from first principles. Because most of the *NN* potentials are semiphenomenological, a choice for restoring gauge invariance has to be made. We adopt the choice of Partovi[20] which is called minimal substitution.[20]

In Sec. II we discuss the impulse approximation (IA), including the Siegert limit, the gauge fixing function, and the relativistic corrections to the one-body charge and current densities. Section III deals with one pion exchange and $\Delta(1232)$ resonance contributions to the charge and current densities. In Sec. IV, the minimal substitution for the nonlocal *NN* potential is discussed. The current density generated from such a procedure is presented in a general manner. Section V contains a discussion of our results and conclusions.

II. IMPULSE APPROXIMATION

For the photonuclear interaction, the Siegert theorem is of prime importance at low energies. The theorem states that

$$\lim_{q_0\to 0} H'_{em} = -\lim_{q_0\to 0}\int d^3x\ \mathbf{A}(\mathbf{x})\cdot[H_0,\mathbf{D}^{(1)}(\mathbf{x})]\ , \tag{2.1}$$

$$\mathbf{D}^{(1)}(\mathbf{x})=\mathbf{x}\rho_{\rm NRIA}(\mathbf{x})\ , \tag{2.2}$$

where H'_{em} is the interaction Hamiltonian of the radiation field with the nucleon system, $\rho_{\rm NRIA}$ is given by (2.3a) below, q_0 is the photon energy, and H_0 is the strong interaction Hamiltonian of the system.

A straightforward calculation of the photonuclear process with the NRIA charge and current density for point nucleons, given by

$$\rho_{\rm NRIA}(\mathbf{x})=\sum_{\alpha=1}^{A} e_\alpha\delta(\mathbf{x}-\mathbf{r}_\alpha)\ , \tag{2.3a}$$

$$\mathbf{J}_{\rm NRIA}(x)=\frac{1}{2m_N}\sum_{\alpha=1}^{A} e_\alpha[\delta(\mathbf{x}-\mathbf{r}_\alpha)\mathbf{p}_\alpha+\mathbf{p}_\alpha\delta(\mathbf{x}-\mathbf{r}_\alpha)] + \frac{e}{2m_N}\sum_{\alpha=1}^{A}\mu_\alpha\nabla_x\delta(\mathbf{x}-\mathbf{r}_\alpha)\times\sigma_\alpha\ , \tag{2.3b}$$

and in the transverse gauge for this radiation field,

$$\mathbf{A}(\mathbf{x})=\epsilon e^{i\mathbf{q}\cdot\mathbf{x}}\ , \tag{2.4a}$$

$$\phi(\mathbf{x})=0\ , \tag{2.4b}$$

does not satisfy the Siegert limit as $q_0\to 0$; it also leads to too small a value for the matrix elements. Meson exchange effects are required to restore gauge invariance. However, meson exchange processes are not well defined with a phenomenological potential. At low energies, it is possible to minimize the effects of meson exchange by use of Siegert's theorem,[21] since the nuclear charge density is known much better than the current density. The two-body contribution to ρ is of order $O(q_0^2/m_N^2)$, where m_N is the nucleon mass, whereas the two-body contribution to $\mathbf{J}$ is of order $O(q_0/m_N)$.

Based on the success of the application of Siegert's theorem, several approaches have been attempted at higher energies (shorter wavelength) where retardation effects become important. These approaches can be classified into two categories: (1) Start with analyzing the radiation field.[2,22] (2) Start with analyzing the current.[23] In this paper we examine these approaches from a gauge transformation point of view.

In quantum electrodynamics (QED) the gauge transformation is

$$\mathbf{A}'=\mathbf{A}+\nabla\Lambda\ ,$$

$$\phi'=\phi-\frac{\partial\Lambda}{\partial t}\ ,$$

$$\psi'-e^{ie\Lambda}\psi\ ,$$

$(\phi,\mathbf{A})$, $(\phi',\mathbf{A}')$ should be understood as the matrix elements of the corresponding field operator between the vacuum state $\langle 0|$ and the transverse photon state $|q\epsilon_\lambda\rangle$, and Λ is an arbitrary function of $\mathbf{x}$; the time dependence, $e^{-i\omega t}$, is suppressed in the following discussion. The interaction Hamiltonian H'_{em} of the nucleon system is invariant under such a transformation

$$H'_{em}=-\int d^3x\ \mathbf{A}^{(T)}(\mathbf{x})\cdot\mathbf{J}(\mathbf{x}) =\int d^3x[-\mathbf{A}'(\mathbf{x})\cdot\mathbf{J}(\mathbf{x})+\phi'(\mathbf{x})\rho(\mathbf{x})]\ , \tag{2.5}$$

where the superscript T on $\mathbf{A}$ indicates it is in the transverse gauge. It is easy to show that if, and only if,

$$\lim_{q_0\to 0}\Lambda(\mathbf{x})=\epsilon\cdot\mathbf{x}\ , \tag{2.6}$$

the nonrelativistic current (2.3) has the Siegert limit expressed by (2.1) and (2.2). In deriving (2.1) we have used the dynamical relation $q_0\mathbf{D}^{(1)}(\mathbf{x})=[H_0,\mathbf{D}^{(1)}(\mathbf{x})]$, which is valid for matrix elements. From (2.4), (2.5), and (2.6) it can be seen that there are an infinite number of gauge choices which lead to a Siegert limit. In principle, it should make no difference for the final result at low energies. However, since in the NRIA J_μ is not necessarily conserved[24] the choice of gauge does become important.

In the following we list several choices for $\Lambda(\mathbf{x})$:

a. Foldy gauge:[22]

$$\Lambda(\mathbf{x})=\epsilon_\lambda\cdot\mathbf{x}\left[\frac{e^{i\mathbf{q}\cdot\mathbf{x}}-1}{i\mathbf{q}\cdot\mathbf{x}}\right] =\epsilon_\lambda\cdot\mathbf{x}\int_0^1 ds\ e^{is\mathbf{q}\cdot\mathbf{x}} \cong\epsilon_\lambda\cdot\mathbf{x}[1+\tfrac{1}{2}i\mathbf{q}\cdot\mathbf{x}-\tfrac{1}{6}(\mathbf{x}\cdot\mathbf{q})^2+O(q_0^3)]\ , \tag{2.7}$$

b. Partovi gauge:[2]

$$\Lambda(\mathbf{x})=\sum_{J,m} D^J_{m,\lambda}(0,-\theta,-\phi)\left[\frac{2\pi(2J+1)}{J(J+1)}\right]^{1/2} \times\frac{i^{J-1}}{q_0}\left[1+x\frac{d}{dx}\right]j_J(q_0x)Y_{Jm}(\hat{x}) \cong\epsilon_\lambda\cdot\mathbf{x}\{1+\tfrac{1}{2}i\mathbf{q}\cdot\mathbf{x}-\tfrac{1}{6}[\mathbf{q}^2x^2+(\mathbf{x}\cdot\mathbf{q})^2]+O(q_0^3)\}\ , \tag{2.8}$$

c. Friar and Fallieros (FF) gauge:[23]

$$\Lambda(\mathbf{x})=\sum_{J,m} D^{J}_{m,\lambda}(0,-\theta,-\phi)\left[\frac{2\pi(2J+1)(J+1)}{J}\right]^{1/2} \times\frac{(iq_0)^{J-1}}{(2J+1)!!}x^J g_J(q_0x)Y_{J_m}(\hat{x}) \cong\epsilon_\lambda\cdot\mathbf{x}[1+\tfrac{1}{2}i\mathbf{q}\cdot\mathbf{x}-\tfrac{1}{6}(\mathbf{x}\cdot\mathbf{q})^2+O(q_0^3)] , \quad (2.9)$$

where λ is the photon helicity (±1) and the special function $g_J(x)$ is defined in Ref. 23. The three gauges of Eqs. (2.7)–(2.9) have the same two leading terms for small q_0. Commonly, the Partovi gauge is used; the Foldy and the FF gauges are the same gauge in different forms; as was pointed out in Ref. 23, they have the good theoretical property that $\mathbf{A}'(\mathbf{x})$ projects out from $\mathbf{J}(\mathbf{x})$ only the magnetic part while other gauges always leave some of the charge part of $\mathbf{J}$, which can be determined from the charge density through the continuity equation,[23] in the $\mathbf{A}'\cdot\mathbf{J}$ term rather than in the charge density. Thus our knowledge of $\rho_{\rm NRIA}$, the nonrelativistic one-body nucleon charge density, is optimized in the FF gauge. The Partovi gauge differs from the other two gauges in terms of order q_0^2 and higher. In Table I we compare, for the Hamada Johnston potential,[25] the reduced electric matrix elements defined by Eq. (52) of Partovi[2] with those computed in the FF gauge; they are quite similar at 20 MeV. From the similarity of the right three and left three columns of Table I we can see that gauge invariance is maintained at small photon energies.

The expressions we used for the electric and magnetic multipole operators $T^{\rm el}_{Jm}(\mathbf{q})$ and $T^{\rm mag}_{Jm}(\mathbf{q})$ in the FF Gauge are

$$T^{\rm el}_{Jm}(q)=\frac{q^{J-1}}{(2J+1)!!}\times\int d^3x\left[i\left[\frac{J+1}{J}\right]^{1/2}\dot{\rho}(\mathbf{x})x^J Y_{Jm}(\hat{x})g_J(qx) +\frac{2q^2}{J+2}\boldsymbol{\mu}(\mathbf{x})\cdot\mathbf{Y}^m_{JJ}(\hat{x})x^J h_J(qx)\right] , \quad (2.10)$$

$$T^{\rm mag}_{Jm}(q)=\int d^3x\,\mathbf{J}(\mathbf{x})\cdot\mathbf{Y}^m_{JJ}(\hat{x})j_J(qx) , \quad (2.11)$$

where $\boldsymbol{\mu}(\mathbf{x})=\frac{1}{2}\mathbf{x}\times\mathbf{J}(\mathbf{x})$, $\dot{\rho}(\mathbf{x})=(d/dt)\rho(\mathbf{x})$, $\mathbf{Y}^m_{JJ}(\hat{x})=1/\sqrt{J(J+1)}\mathbf{L}Y_{Jm}$, $\mathbf{L}=-i\mathbf{x}\times\nabla_x$. For the NRIA charge and current densities (3.3), (2.10) becomes

$$T^{\rm el}_{Jm}(q)=\frac{q^{J-1}}{(2J+1)!!}\left\{-q\left[\frac{J+1}{J}\right]^{1/2}\left[\frac{r}{2}\right]^J g_J(\tfrac{1}{2}qr)Y_{Jm}+\frac{q^2}{4m_N}\frac{\sqrt{J(J+1)}}{J+2}\left[\frac{r}{2}\right]^J h_J(\tfrac{1}{2}qr)Y_{Jm} +\frac{q^2}{2m_N}\frac{1}{J+2}\left[\frac{r}{2}\right]^J h_J(\tfrac{1}{2}qr)[Y_J\otimes L]^J_m +\frac{\mu^{s/v}q^2}{2m_N}\frac{1}{J+2}\left[\left[\frac{r}{2}\right]^J r\frac{d}{dr}h_J(\tfrac{1}{2})+(J+2)\left[\frac{r}{2}\right]h_J(\tfrac{1}{2}qr)\right][Y_J\otimes\Sigma]^J_m\right\} . \quad (2.12)$$

TABLE I. Reduced matrix elements in FF (left) and Partovi (right) gauge. In this table, L is the multipole order, j is the final-state total angular momentum, and λ labels different couplings.

	FF gauge $T^{(L)}(\lambda j)(10^{-3}$ Fermi)				Partovi gauge $T^{(L)}(\lambda j)(10^{-3}$ Fermi)		
$Lj\lambda$	20 MeV	40 MeV	140 MeV	$Lj\lambda$	20 MeV	40 MeV	140 MeV
103	−11.52	−2.28	−1.47	103	−11.58	−2.39	−1.53
112	−0.26	−0.37	−0.37	112	−0.25	−0.37	−0.38
114	38.83	14.95	8.59	114	39.05	15.53	9.09
121	−33.31	−3.35	1.34	121	−33.59	−4.36	−0.06
123	21.25	13.56	10.94	123	21.47	13.94	11.35
211	−0.03	0.00	0.01	211	−0.03	0.04	0.14
213	−1.76	−1.39	−1.17	213	−1.78	−1.34	−1.04
222	−0.12	−0.37	−0.43	222	−0.12	−0.37	−0.41
224	2.84	1.62	0.97	224	2.86	1.65	0.76
231	−2.61	−2.53	−2.07	231	−2.64	−2.54	−1.99
233	−1.50	−0.17	0.39	233	−1.52	−0.13	0.58
321	−0.05	−0.07	−0.08	321	−0.05	−0.05	−0.05
323	−0.16	−0.29	−0.37	323	−0.17	−0.23	−0.26
332	−0.00	−0.01	−0.03	332	−0.00	−0.01	−0.02
334	0.23	0.46	0.56	334	0.24	0.38	0.45
341	−0.13	−0.03	−0.01	341	−0.13	0.03	0.09
343	0.19	0.48	0.74	343	0.19	0.47	0.77

the tensor operator $[T^{k_1}_{q_1}\otimes T^{k_2}_{q_2}]^J_m$ of rank J is defined as

$$[T^{k_1}\otimes T^{k_2}]^J_m=\sum_{q_1q_2}\langle k_1q_1;k_2q_2\,|\,Jm\rangle T^{k_1}_{q_1}T^{k_2}_{q_2}\ .$$

The quantity Σ in Eq. (2.12) is $\Sigma=S_1+S_2$ or S_1-S_2 depending on the transition, $g_J(x)$ and $h_J(x)$ are defined in Ref. 23, $\langle k_1q_1;k_2q_2\,|\,Jm\rangle$ is a Clebsch-Gordan coefficient, and $T^{k_1}_{q_1}, T^{k_2}_{q_2}$ are tensor operators of rank k_1,k_2, respectively. The reduced matrix element of $T^{\rm el}_{Jm}$ and its relationship with the cross section are given in Appendix A and that of $T^{\rm mag}_{Jm}$ can be found, e.g., in Ref. 2. The relativistic correction to the charge and current densities needs to be included, and leads to an important reduction of the forward differential cross section. There are two kinds of relativistic corrections: (1) terms generated from the spinor reduction of the charge and density operators (FW transformation), and (2) terms generated from the boosting of the initial deuteron wave function from the rest frame to the c.m. frame of the reaction in which the deuteron moves with a velocity q/M_D. This transformation can be treated effectively as an additional current density between the initial and the final state wave functions in the c.m. system. For a low-energy process, the second correction is expected to be very small. Therefore, only the first part of the relativistic correction is considered in this paper. The coordinate space charge and current densities to $O(m^{-2})$ in the c.m. systems are

$$\rho^{RC}(\mathbf{x})=\rho_1^{RC}(\mathbf{x})+\rho_2^{RC}(\mathbf{x})\ ,$$
$$\mathbf{J}^{RC}(\mathbf{x})=\mathbf{J}_1^{RC}(\mathbf{x})+\mathbf{J}_2^{RC}(\mathbf{x})\ , \tag{2.13}$$

with

$$\rho_1^{RC}(\mathbf{x})=e_1\frac{\nabla_x^2}{8m_N^2}\delta\left(\mathbf{x}-\frac{\mathbf{r}}{2}\right)+\frac{2\kappa_1+e_1}{4m_N^2}\nabla_x\delta\left(\mathbf{x}-\frac{\mathbf{r}}{2}\right)\cdot\boldsymbol{\sigma}_1\times\mathbf{p}\ , \tag{2.13a}$$

$$\mathbf{J}_1^{RC}(\mathbf{x})=-\frac{q\kappa_1}{4m_N^2}\left[i\nabla_x\delta\left(\mathbf{x}-\frac{\mathbf{r}}{2}\right)+2\delta\left(\mathbf{x}-\frac{\mathbf{r}}{2}\right)i\boldsymbol{\sigma}_1\times\mathbf{p}\right]$$
$$+\frac{e_1}{4m_N^3}\left[-2\delta\left(\mathbf{x}-\frac{\mathbf{r}}{2}\right)\mathbf{p}\mathbf{p}^2+\nabla_x\delta\left(\mathbf{x}-\frac{\mathbf{r}}{2}\right)\cdot\mathbf{p}\boldsymbol{\sigma}_1\times\mathbf{p}+\boldsymbol{\sigma}_1\times\nabla_x\delta\left(\mathbf{x}-\frac{\mathbf{r}}{2}\right)\mathbf{p}^2\right]-\frac{\kappa_1}{4m_N^3}\nabla_x\delta\left(\mathbf{x}-\frac{\mathbf{r}}{2}\right)\mathbf{p}\boldsymbol{\sigma}_1\cdot\mathbf{p}\ , \tag{2.13b}$$

and where $\mathbf{p}=-i\nabla$, $e_i=\frac{1}{2}(1+\tau_{iz})$, $\kappa_i=\frac{1}{2}(\kappa_s+\kappa_v\tau_{iz})$, $1+\kappa_s=\mu_p+\mu_n, 1+\kappa_v=\mu_p-\mu_n$. The quantities ρ_2^{RC} and $\mathbf{J}_2^{RC}$ are obtained from Eqs. (2.13a) and (2.13b) by the transformation $1\to2$, $\mathbf{r}\to-\mathbf{r}$, and $\mathbf{p}\to-\mathbf{p}$. The c.m. coordinate has been removed from the δ function; it gives total momentum conservation. The first term in ρ is known as the Darwin-Foldy term and the second one as the spin-orbit term. For a detailed multipole analysis in the long wavelength limit, we refer the reader to Appendix C of Ref. 26.

III. ONE PION AND Δ(1232) CONTRIBUTIONS

Both pion and Δ(1232) current contributions are important for a consistent and reliable treatment of the electromagnetic interaction with the nuclear system. As has been discussed in Sec. II, the two-body contribution to the charge density is of $O(m_N^{-1})$ times smaller than to the current density. Thus in considering these terms, more care has to be taken in order to keep the calculation consistent. In the PV coupling scheme the pion contribution is expressed by the diagrams of Fig. 1.

The pion current is the summation of the seagull contribution, Figs. 1(a) and 1(b) and the pion current contribution, Fig. 1(c)

$$\mathbf{J}_\pi^{\rm PV}=\mathbf{J}(SG)+\mathbf{J}(\pi C)\ . \tag{3.1}$$

In the c.m. system, to leading order in m_N^{-1} these currents are

$$\mathbf{J}(SG)=-i\frac{f^2_{\pi NN}}{m_\pi^2}(\boldsymbol{\tau}_1\times\boldsymbol{\tau}_2)_z$$
$$\times\left[\frac{\boldsymbol{\sigma}_1(\boldsymbol{\sigma}_2\cdot\mathbf{k}_2)}{\omega^2(\mathbf{k}_2)-\frac{1}{4}q_0^2}-\frac{\boldsymbol{\sigma}_2(\boldsymbol{\sigma}_1\cdot\mathbf{k}_1)}{\omega^2(\mathbf{k}_1)-\frac{1}{4}q_0^2}\right]\ , \tag{3.2}$$

$$\mathbf{J}(\pi C)=i\frac{f^2_{\pi NN}}{m_\pi^2}(\boldsymbol{\tau}_1\times\boldsymbol{\tau}_2)_z\frac{\boldsymbol{\sigma}_1\cdot\mathbf{k}_1\boldsymbol{\sigma}_2\cdot\mathbf{k}_2}{[(\omega^2(\mathbf{k}_1)-\frac{1}{4}q_0^2)][\omega^2(\mathbf{k}_2)-\frac{1}{4}q_0^2)]}$$
$$\times(\mathbf{k}_1-\mathbf{k}_2)\ , \tag{3.3}$$

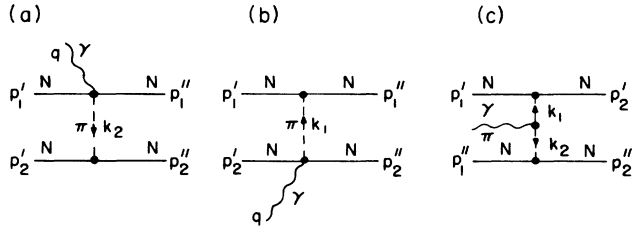

FIG. 1. One pion exchange contribution to J^μ_{em}. (a) and (b) are the seagull term contributions and (c) is the pion current contribution.

where $\mathbf{k}_1=\mathbf{p}_1''-\mathbf{p}_1'$, $\mathbf{k}_2=\mathbf{p}_2''-\mathbf{p}_2'$, and $\mathbf{p}_i''(\mathbf{p}_i')$ are the final (initial) momentum of the ith nucleon, $\omega^2(\mathbf{k})=\mathbf{k}^2+m_\pi^2$; the $-\frac{1}{4}q_0^2$ term in the denominator is an approximation that results from the on-shell treatment of the nucleon in the deuteron. We expand $J(SG)$ and $J(\pi C)$ in terms of the photon energy q_0, keep only terms up to $O(q_0^2)$, and use variables $\mathbf{p},\mathbf{q}$ which are related to $\mathbf{k}_1,\mathbf{k}_2$ by

$$\mathbf{k}_1=\mathbf{p}+\frac{\mathbf{q}}{2}\ ,$$

$$\mathbf{k}_2=-\mathbf{p}+\frac{\mathbf{q}}{2}\ ,$$

where $\mathbf{q}$ is the momenta of the photon and $\mathbf{p}$ is the difference between final and initial relative momenta of the two nucleons. The result of the expansion is

$$\begin{aligned}\mathbf{J}(SG)=&\frac{f_{\pi NN}^2}{m_\pi^2}i(\tau_1\times\tau_2)_z\{(\sigma_1\sigma_2\cdot\mathbf{p}+\sigma_2\sigma_1\cdot\mathbf{p})[\omega^{-2}(\mathbf{p})+\tfrac{1}{4}(q_0^2-\mathbf{q}^2)\omega^{-4}(\mathbf{p})+(\mathbf{p}\cdot\mathbf{q})^2\omega^{-6}(\mathbf{p})]\\&+(\sigma_1\sigma_2\cdot\mathbf{p}-\sigma_1\cdot\mathbf{p}\sigma_2)\mathbf{p}\cdot\mathbf{q}\omega^{-4}(\mathbf{p})-\tfrac{1}{2}(\sigma_1\sigma_2\cdot\mathbf{p}-\sigma_2\sigma_1\cdot\mathbf{p})\omega^{-2}(\mathbf{p})\\&-\tfrac{1}{2}(\sigma_1\sigma_2\cdot\mathbf{q}+\sigma_1\cdot\mathbf{q}\sigma_2)\mathbf{p}\cdot\mathbf{q}\omega^{-4}(\mathbf{p})\}\ ,\end{aligned}\tag{3.4}$$

$$\begin{aligned}\mathbf{J}(\pi C)=&-\frac{2f_{\pi NN}^2}{m_\pi^2}i(\tau_1\times\tau_2)_z\mathbf{p}\{[\sigma_1\cdot\mathbf{p}\sigma_2\cdot\mathbf{p}-\tfrac{1}{2}(\sigma_1\cdot\mathbf{p}\sigma\cdot\mathbf{q}-\sigma_1\cdot\mathbf{q}\sigma_2\cdot\mathbf{p})-\tfrac{1}{4}\sigma_1\cdot\mathbf{q}\sigma_2\cdot\mathbf{q}]\omega^{-4}(\mathbf{p})\\&+\tfrac{1}{2}\sigma_1\cdot\mathbf{p}\sigma_2\cdot\mathbf{p}(q_0^2-\mathbf{q}^2)\omega^{-6}(\mathbf{p})+\sigma_1\cdot\mathbf{p}\sigma_2\cdot\mathbf{p}(\mathbf{p}\cdot\mathbf{q})^2\omega^{-8}(\mathbf{p})\}\ .\end{aligned}\tag{3.5}$$

Following Ref. 26, the one pion exchange charge density with PV coupling in the quasipotential formalism is

$$\begin{aligned}\rho(1\pi E)=&\rho(SG)+\rho(\pi C)+\Delta\rho_1+\Delta\rho_2\\=&\frac{f_{\pi NN}^2}{4m_N m_\pi^2}\{\tau_1\cdot\tau_2\omega^{-2}(\mathbf{p})(\sigma_1\cdot\mathbf{p}\sigma_2\cdot\mathbf{q}-\sigma_1\cdot\mathbf{q}\sigma_2\cdot\mathbf{p})\\&+\tfrac{1}{2}(\tau_{1z}+\tau_{2z})\omega^{-2}(\mathbf{p})(\sigma_1\cdot\mathbf{p}\sigma_2\cdot\mathbf{q}-\sigma_1\cdot\mathbf{q}\sigma_2\cdot\mathbf{p})+\tfrac{1}{2}(\tau_{1z}-\tau_{2z})\omega^{-2}(\mathbf{p})(\sigma_1\cdot\mathbf{p}\sigma_2\cdot\mathbf{q}+\sigma_1\cdot\mathbf{q}\sigma_2\cdot\mathbf{p})\\&+\tfrac{1}{4}(\tau_{1z}-\tau_{2z})[\omega^{-2}(\mathbf{p})(\sigma_1\cdot\mathbf{p}\sigma_2\cdot\mathbf{q}+\sigma_1\cdot\mathbf{q}\sigma_2\cdot\mathbf{p})-2\omega^{-4}(\mathbf{p})\sigma_1\cdot\mathbf{p}\mathbf{p}\cdot\mathbf{q}]\\&-\tfrac{1}{2}i(\tau_1\times\tau_2)_z\omega^{-2}(\mathbf{p})[\sigma_1\cdot\mathbf{q}\sigma_2\cdot(2\mathbf{p}'+\mathbf{p})+\sigma_1\cdot(2\mathbf{p}'+\mathbf{p})\sigma_2\cdot\mathbf{q}]\\&+i(\tau_1\times\tau_2)_z\omega^{-4}(\mathbf{p})[2\mathbf{p}\cdot\mathbf{q}(\sigma_1\cdot\mathbf{p}\sigma_2\cdot\mathbf{p}+\sigma_1\cdot\mathbf{p}'\sigma_2\cdot\mathbf{p}+\sigma_1\cdot\mathbf{p}\sigma_2\cdot\mathbf{p}')-\sigma_1\cdot\mathbf{p}\sigma_2\cdot\mathbf{p}(2\mathbf{p}'+\mathbf{p})\cdot q]\}\\&+(f_{\pi NN}^2/m_\pi^2)i(\tau_1\times\tau_2)_z\tfrac{1}{4}q_0[\omega^{-4}(\mathbf{p})(\sigma_1\cdot\mathbf{p}\sigma_2\cdot\mathbf{q}+\sigma_1\cdot\mathbf{q}\sigma_2\cdot\mathbf{p})-4\omega^{-4}(\mathbf{p})\sigma_1\cdot\mathbf{p}\sigma_2\cdot\mathbf{p}\mathbf{p}\cdot\mathbf{q}]\ .\end{aligned}\tag{3.6}$$

Here $\rho(SG)$ and $\rho(\pi C)$ come directly from the diagrams of Fig. 1, $\Delta\rho_2$ is the piece of the effective 1π charge density that results from the 2π exchange contributions in the quasi-potential formalism, part of which is important for the conservation of the total current (See Refs. 11 and 26), and $\Delta\rho_1$ is the effective charge density resulting from the perturbative modification of the 1π part of the potential (Bonn potential in this paper) by adding the terms of order m_N^{-2} in the 1π exchange potential between nucleons.[11]

The $\Delta(1232)$ contribution to the current is expressed diagrammatically in Fig. 2. The Δ propagator used in this paper takes the form[27,28]

$$D_{\mu\nu}=\frac{i(\gamma\cdot p+m_\Delta)}{p^2-m_\Delta^2+i\epsilon}\Lambda_{\mu\nu}\ ,\tag{3.7}$$

$$\Lambda_{\mu\nu}=\left[-g_{\mu\nu}+\tfrac{1}{3}\gamma_\mu\gamma_\nu+\frac{1}{3p^2}(\gamma\cdot p\gamma_\mu p_\nu+p_\mu\gamma_\nu\gamma\cdot p)\right]\ .\tag{3.8}$$

The $\gamma N\to\Delta$ vertex[6] is

$$\Gamma_{\lambda\nu}^{\gamma N\Delta}=-ie\frac{f_{\gamma N\Delta}}{m_\pi}(\gamma_\lambda q_\nu-\gamma\cdot q g_{\lambda\nu})\gamma_5\ ,\tag{3.9}$$

and the $\Delta\to N\pi$ vertex[6] is

$$\Gamma_\mu^{\Delta\pi N}=-\frac{f_{\Delta\pi N}}{m_\pi}k_\mu\ ,\tag{3.10}$$

where p, q, and k are the 4 momenta of Δ, γ, and π. For simplicity the isospin operators have been suppressed in Eqs. (3.7)–(3.10). There are no contributions from Figs. 2(a) and 2(b) because the initial deuteron has total isospin zero; thus only Figs. 2(c) and 2(d) are needed. The current and charge densities in the c.m. system follow from the Δ propagator

and vertices. After making the spinor reduction, keeping only the leading order terms in m_N^{-1} and in m_Δ^{-1} but quadratic in $\mathbf{q}$ and q_0, we obtain

$$\mathbf{J}(\Delta)=\frac{f_{\pi NN}f_{\pi N\Delta}f_{\gamma N\Delta}}{m_\pi^3 m_\Delta}\tfrac{2}{3}(\tau_{1z}-\tau_{2z})\left[1-\frac{2m_N q_0}{m_\Delta^2-m_N^2}\right]^{-1}$$
$$\times\{\omega^{-2}(\mathbf{p})[-ai\mathbf{q}\times\mathbf{p}(\sigma_1-\sigma_2)\cdot\mathbf{p}-b\mathbf{p}\cdot\mathbf{q}(\sigma_1\sigma_2\cdot\mathbf{p}-\sigma_1\cdot\mathbf{p}\sigma_2)+b\mathbf{p}(\sigma_1\cdot\mathbf{q}\sigma_2\cdot\mathbf{p}-\sigma_1\cdot\mathbf{p}\sigma_2\cdot\mathbf{q})]$$
$$+\omega^{-2}(\mathbf{p})[-\tfrac{1}{2}ai\mathbf{q}\times\mathbf{p}(\sigma_1+\sigma_2)\cdot\mathbf{q}+\tfrac{1}{2}b\mathbf{p}\cdot\mathbf{q}(\sigma_1\sigma_2\cdot\mathbf{q}+\sigma_1\cdot\mathbf{q}\sigma_2)$$
$$-b\mathbf{p}\sigma_1\cdot\mathbf{q}\sigma_2\cdot\mathbf{q}-\tfrac{1}{2}b\mathbf{q}(\sigma_1\cdot\mathbf{q}\sigma_2\cdot\mathbf{p}+\sigma_1\cdot\mathbf{p}\sigma_2\cdot\mathbf{q})+\tfrac{1}{2}(b\mathbf{q}^2-2bq_0^2)(\sigma_1\sigma_2\cdot\mathbf{p}+\sigma_1\cdot\mathbf{p}\sigma_2)]$$
$$+\omega^{-4}(\mathbf{p})[a\mathbf{p}\cdot\mathbf{q}(i\mathbf{q}\times\mathbf{p})(\sigma_1+\sigma_2)\cdot\mathbf{p}-b(\mathbf{p}\cdot\mathbf{q})^2(\sigma_1\sigma_2\cdot\mathbf{p}+\sigma_1\cdot\mathbf{p}\sigma_2)+b\mathbf{p}(\mathbf{p}\cdot\mathbf{q})(\sigma_1\cdot\mathbf{q}\sigma_2\cdot\mathbf{p}+\sigma_1\cdot\mathbf{p}\sigma_2\cdot\mathbf{q})]\}\ , \tag{3.11}$$

and

$$\rho(\Delta)=\frac{f_{\pi NN}f_{\pi N\Delta}f_{\gamma N\Delta}}{m_\pi^3 m_N m_\Delta}\tfrac{2}{3}(\tau_{1z}-\tau_{2z})\left[1-\frac{2m_N q_0}{m_\Delta^2-m_N^2}\right]^{-1}$$
$$\times\omega^{-2}(\mathbf{p})[ai\mathbf{q}\cdot(\mathbf{p}\times\mathbf{p}')(\sigma_1+\sigma_2)\cdot\mathbf{p}-b\mathbf{p}\cdot\mathbf{q}(\sigma_1\cdot\mathbf{p}'\sigma_2\cdot\mathbf{p}+\sigma_1\cdot\mathbf{p}\sigma_2\cdot\mathbf{p}')-(-b\mathbf{p}'\cdot p+e\mathbf{p}^2)$$
$$\times(\sigma_1\cdot\mathbf{q}\sigma_2\cdot\mathbf{p}+\sigma_1\cdot\mathbf{p}\sigma_2\cdot\mathbf{q})-d\mathbf{p}\cdot\mathbf{q}\sigma_1\cdot\mathbf{p}\sigma_2\cdot\mathbf{p}-bq_0m_N(\sigma_1\cdot\mathbf{q}\sigma_2\cdot\mathbf{p}+\sigma_1\cdot\mathbf{p}\sigma_2\cdot\mathbf{q})]\ , \tag{3.12}$$

where

$$a=\frac{2}{3}\left[1-\frac{m_N}{m_\Delta}\right]^{-1},\quad b=-\frac{1}{3}\left[1-\frac{m_N}{m_\Delta}\right]^{-1},$$
$$d=-\left[1+\frac{m_N}{m_\Delta}\right]^{-1},\quad e=\frac{1}{6}\left[1+\frac{m_N}{m_\Delta}\right]^{-1}.$$

The multipole decomposition of the charge and current densities (3.4), (3.5), (3.6), (3.11), and (3.12) are given in detail in Ref. 26. [There is a misprint in Eq. (2.15) of that reference. The sign for the term linear in $\mathbf{q}$ should be reversed.]

IV. MINIMAL SUBSTITUTION IN NONLOCAL ISOSPIN DEPENDENT POTENTIALS

The electromagnetic interaction of the nucleon can be generated by the minimal substitution $\partial_\mu\to\partial_\mu+ieA_\mu$ in the nuclear Lagrangian of the model. Gauge invariance is guaranteed by such a substitution. However, most of the realistic NN potentials are not derived from a fundamental Lagrangian, but are, at least partially, phenomenological in nature. The nonlocality of the potential at short distance breaks gauge invariance and it is necessary to restore it in a reasonable way. In the case of a single particle moving in an external nonlocal potential, the nonlocality of the potential can be related to a momentum dependence through

$$O(\mathbf{r},\mathbf{p})=\int d^3r''d^3r'\delta(\mathbf{r}-\mathbf{r}'')O(\mathbf{r}'',\mathbf{r}')$$
$$\times\exp[i\mathbf{p}\cdot(\mathbf{r}'-\mathbf{r}'')]\ , \tag{4.1}$$

where $\mathbf{p}$ in the exponent is the momentum operator, i.e., $\mathbf{p}=-i\nabla$. With the minimal substitution $\mathbf{p}\to\mathbf{p}-\hat{e}\hat{A}(\mathbf{r})$ in the exponent and use of the Baker-Hausdorf formula

$$e^{\hat{A}+\hat{B}}=e^{\hat{A}}S\exp\left[\int_0^1 ds\, e^{-s\hat{A}}\hat{B}e^{s\hat{A}}\right],$$

where the symbol S stands for ordering of the operators, in the expansion of the exponential, one obtains the gauge invariant operator corresponding to O, namely $\tilde{O}$

$$\tilde{O}(\mathbf{r},\mathbf{p})=\int d^3x\ \delta(\mathbf{x}-\mathbf{r})O(\mathbf{r},\mathbf{p})\exp\left[i\hat{e}\int_{\mathbf{r}}^{\mathbf{x}}\mathbf{A}(\mathbf{x}')\cdot d\mathbf{x}'\right], \tag{4.2}$$

or

$$\tilde{O}(\mathbf{r}'',\mathbf{r}')=O(\mathbf{r}'',\mathbf{r}')\exp\left[i\hat{e}\int_{\mathbf{r}'}^{\mathbf{r}''}\mathbf{A}(\mathbf{x}')\cdot d\mathbf{x}'\right], \tag{4.3}$$

with $\hat{e}=P_3e$, $P_3=\frac{1}{2}(1+\tau_3)$.

The form of (4.2) is convenient to use whereas (4.3) is conceptually transparent. The path of the line integral is arbitrary. The minimal substitution corresponds to the choice of a straight line between the two end points.

However, there are problems with the above procedure. If the operator O is not diagonal in isospin space, (4.2) and (4.3) will no longer be gauge invariant. Partovi has shown[20] that if one removes the isospin projection operator P_3 from $\hat{e}$ and multiplies the end points of the line integral by P_3, then the resulting operator is gauge invariant regardless of the isospin dependence of the operator. We therefore write

$$\tilde{O}(\mathbf{r},\mathbf{p})=\int d^3x\ \delta(\mathbf{x}-P_3\mathbf{r})O(\mathbf{r},\mathbf{p})$$
$$\times\exp\left[ie\int_{P_3\mathbf{r}}^{\mathbf{x}}\mathbf{A}(\mathbf{x}')\cdot d\mathbf{x}'\right], \tag{4.4}$$

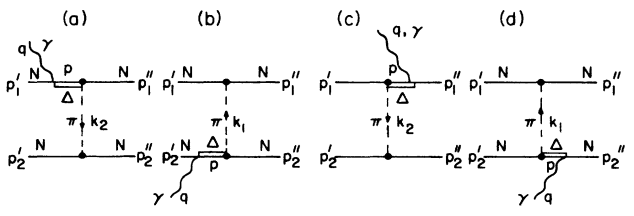

FIG. 2. $\Delta(1232)$ contributions to J^μ_{em}.

or

$$\tilde{O}(\mathbf{r}'',\mathbf{r}')=O(\mathbf{r}'',\mathbf{r}')\exp\left[ie\int_{P_3^r\mathbf{r}'}^{P_3'\mathbf{r}''}\mathbf{A}(\mathbf{x}')\cdot d\mathbf{x}'\right]. \tag{4.5}$$

In (4.5) P_3' acts to the left and P_3^r acts to the right. Applying (4.4) to the nonrelativistic kinetic operator $T=\mathbf{p}^2/2m$ we get the convectional contribution to (2.3) for a linear approximation in **A**, except for the spin contributions in **J**.

The current generated by the two-body isospin dependent potential is given by Eq. (35) of Ref. 20. It takes the form

$$\mathbf{J}(\mathbf{x})=ie\int d^3y\left\{\int_{1/2P_3^{(1)}\mathbf{r}}^{\mathbf{y}}\delta(\mathbf{x}-\mathbf{x}')d\mathbf{x}'[V,\delta(\mathbf{y}-\tfrac{1}{2}P_3^{(1)}\mathbf{r})]+\int_{-1/2P_3^{(2)}\mathbf{r}}^{\mathbf{y}}\delta(\mathbf{x}-\mathbf{x}')\times d\mathbf{x}'[V,\delta(\mathbf{y}+\tfrac{1}{2}P_3^{(2)}\mathbf{r})]\right\} \tag{4.6}$$

in the linear approximation in **A**, where $P_3^{(1)}=\frac{1}{2}(1+\tau_3^{(1)})$, $P_3^{(2)}=\frac{1}{2}(1+\tau_3^{(2)})$. The c.m. coordinate has been taken to be zero in (4.6).

The final and initial states are given by $\chi_f=|pn\rangle$ and $\chi_i=1/\sqrt{2}(|pn\rangle-|np\rangle)$. If the momentum dependence of the nonlocal part of the *NN* potential is expanded to order $O(\mathbf{p}^2)$, it has the general form

$$\Delta V(\mathbf{r},\mathbf{p})=\nabla^2 O(\mathbf{r})+O(\mathbf{r})\nabla^2+O^{LS}(\mathbf{r})\mathbf{L}\cdot\mathbf{S}\,, \tag{4.7a}$$

$$O(\mathbf{r})=O_1(\mathbf{r})+O_2(\mathbf{r})\tau_1\cdot\tau_2\,, \tag{4.7b}$$

$$O^{LS}(\mathbf{r})=O_1^{LS}(\mathbf{r})+O_2^{LS}(\mathbf{r})\tau_1\cdot\tau_2\,, \tag{4.7c}$$

where **L** is the angular momentum operator and **S** is the total spin operator.

The isospin dependence in (4.7b) and (4.7c) is obtained from charge independence of the *NN* interaction. A little algebra converts (4.6) to

$$\mathbf{J}(\mathbf{x})=\frac{ie}{\sqrt{2}}\left[\frac{d}{dr}\tilde{O}(r)\hat{n}_r+2\tilde{O}(r)\nabla+i\tilde{O}^{LS}(r)\mathbf{S}\times\mathbf{r}\right]\delta\left[\mathbf{x}-\frac{\mathbf{r}}{2}\right], \tag{4.8a}$$

$$\tilde{O}(r)=3O_2(r)\,, \tag{4.8b}$$

$$\tilde{O}^{LS}(r)=3O_2^{LS}(r)\,. \tag{4.8c}$$

The multipole decomposition of (4.8a) in the FF gauge gives

$$T_{Jm}^{\mathrm{el}}(q)=-\frac{q^{J+1}}{\sqrt{2}(J+2)(2J+1)!!}\left\{\tilde{O}(r)\left[\frac{r}{2}\right]^J h_J(\tfrac{1}{2}qr)[Y_J\otimes L]_m^J+2\tilde{O}^{LS}(r)\left[\frac{r}{2}\right]^{J+2}h_J(\tfrac{1}{2}qr)[Y_J\otimes S]_m^J\right\}, \tag{4.9}$$

$$T_{Jm}^{\mathrm{mag}}(q)=-\frac{i\sqrt{4\pi}}{\sqrt{3J(J+1)}}\left\{2\frac{\tilde{O}(r)}{r}j_J(\tfrac{1}{2}qr)[Y_J\otimes[Y_1\otimes L]_1]_m^J+\tilde{O}^{LS}(r)rj_J(\tfrac{1}{2}qr)[Y_J\otimes[Y_1\otimes S]_1]_m^J\right\}. \tag{4.10}$$

The reduced matrix elements of T_{Jm}^{el} and T_{Jm}^{mag} are given in Appendix B.

V. RESULTS AND DISCUSSION

In the nonrelativistic impulse approximation, the different gauges in which we perform the calculation affect the final results because the IA is not current conserving. A comparison of the forward differential cross section in the Partovi and FF gauges are shown in Fig. 3. The difference vanishes at small photon energies and is of order q_0^2 and higher [see Eqs. (2.8) and (2.9)]. The difference does not disappear when the meson exchange contributions are included. One reason is that the matrix element for meson exchange is evaluated in the long wavelength approximation, i.e., $j_L(x)\to 1/(2L+1)x^L$, when the multipole decomposition is made. Therefore, only the leading term in q_0 of each multipole operator for the meson exchange contribution is considered. We keep terms up to $L=4$ in our numerical work. The other reason is that the current is expanded in a power series in q_0 and only terms of order q_0^2 term and lower are kept. So we do not expect the differences of order q_0^2 and higher between the two gauges to diminish when meson exchange effects are included. The difference may be regarded as a rough estimate of the theoretical uncertainty of our calculation. The FF gauge gives lower values for the forward differential cross section, closer to experiment. Due to this practical advantage and the theoretical advantages discussed in Ref. 18 and Sec. II of this paper, we suggest use of the FF gauge in future calculations of the electromagnetic interaction with nucleons and nuclei especially when only a simple IA is employed for small or moderate momentum transfers.[43] This argument is strengthened by recent work, e.g., FF.[44]

One reason for undertaking this work was the belief that a reduction in the *D*-state probability might resolve the discrepancy between the theoretical and experimental forward differential cross section. This is suggested by the work of Ref. 6. Thus it was hoped that the use of the Bonn potential, which has a smaller *D*-state probability, would produce a theoretical cross section closer to experiment. We find little dependence on the *D*-state probability for a fixed asymptotic *D*/*S* ratio of 0.026. From Fig. 4 it can be seen that, when all of the corrections are included, the final result is almost identical with that of the Paris potential of Ref. 26, which has the same asymptotic *D*/*S* ratio. Thus, despite the suggestions of Ref. 6, the forward differential cross section is not very sensitive to the *D*-state probability of the deuteron. Indeed, other re-

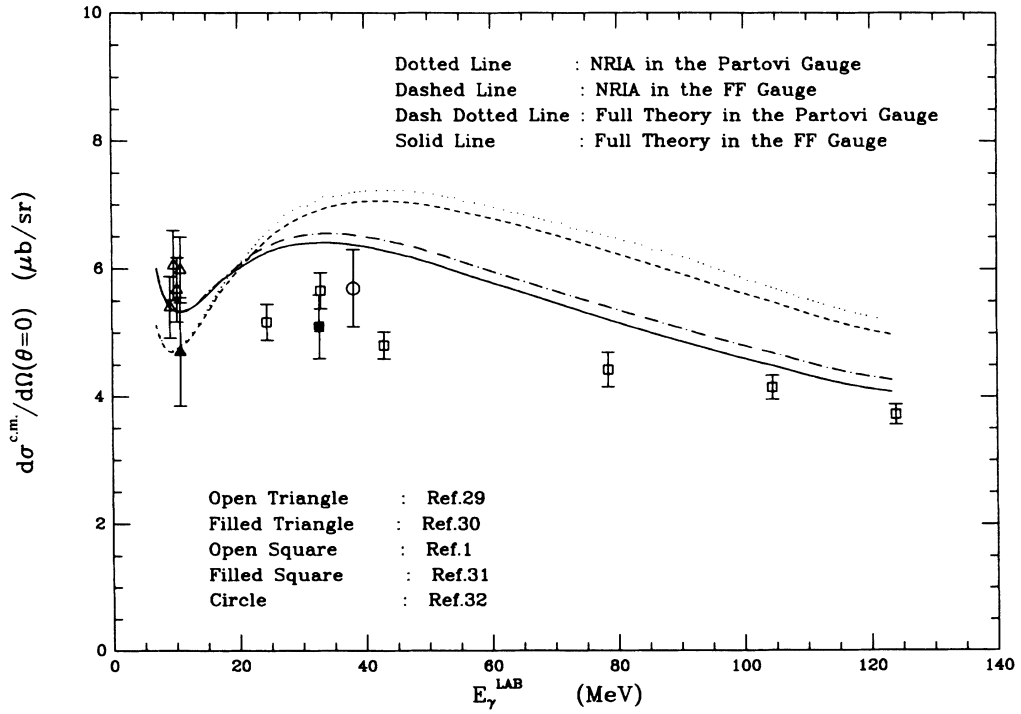

FIG. 3. Comparison between the FF gauge and the Partovi gauge. The dotted line is calculated in the Partovi gauge in NRIA; the dashed line is calculated in the FF gauge in NRIA; the dash-dotted line is calculated in the Partovi gauge with relativistic corrections (RC), meson-exchange corrections (MEC), Δ, and gauge corrections taken into account. The solid line is calculated in the FF gauge with RC, MEC, Δ, and gauge corrections taken into account. Open triangle points are from Ref. 29, filled triangle points are from Ref. 30, open square points are from Ref. 1, filled square points are from Ref. 31 and circle points are from Ref. 32.

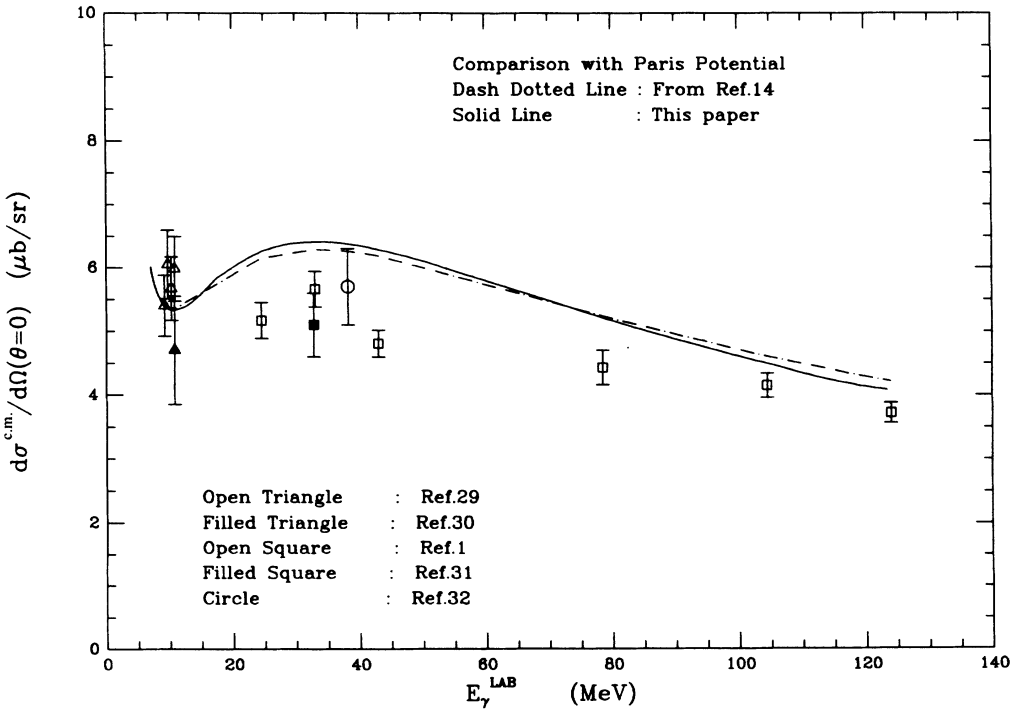

FIG. 4. Comparison between the Paris potential and the Bonn potential calculation. Experimental data points are the same as Fig. 1. The dash-dotted curve is from Ref. 11 and the solid curve is the result of this paper with RC, MEC, Δ, and gauge corrections taken into account.

cent studies confirm this finding; in Ref. 18 the forward differential cross sections for various potentials are found to be insensitive to the potential choice when the wave function of the deuteron is adjusted to fit static properties, including the asymptotic D/S ratio. The reason for this insensitivity is that the matrix elements of the electromagnetic interaction at low energies depend only on the low order multipoles, i.e., $(E1, M1, E2\ldots)$. Among these, only $M1$, which is not very important in our approach and in the energy range considered in this work, is sensitivity to the short-range part of the deuteron wave function, because it connects initial to final S states. We have made a numerical comparison of the reduced electric and magnetic matrix elements between the Bonn and the Hamada Johnston potentials; the results confirm the argument. In addition it shows that for the same multipole, e.g., $E1$ or $M1$, the difference is larger for those final states coupled by tensor forces than for the uncoupled ones. However the work of Leidemann and Arenhövel[45] has a much larger (by more than a factor of 2 at our highest energy) $M1$ contribution and this increase may account for the larger sensitivity to P_D obtained by Wilhelm, Leidemann, and Arenhövel.[46]

In Fig. 5 we present our theoretical curves with various corrections added step by step in the FF gauge. The minimal substitution in the nonlocal part of the Bonn potential does not make a significant contribution. As can be seen from Fig. 5, the absence of this term is indistinguishable from the solid curve. The solid curve for the forward differential cross section as a function of photon energy is higher between 20 to 80 MeV and lower for higher or lower energies than that of Ref. 6, but it qualitatively agrees with the results of Ref. 18 at all energies. Our final solid curve calculated in the Bonn potential shows that the discrepancy between theory and experiment remains a mystery.

In Figs. 6–9 the results for the angular distribution at energies of 30, 60, 100, and 140 MeV are presented. The experimental data are the same as Ref. 6. One can see that theory and experiment are quite close together, for $E_\gamma \leq 100$ MeV. At $E_\gamma \approx 140$ MeV the agreement becomes poor. This is in contrast to a recent publication by Leidemann and Arenhövel,[45] who find that inclusion of the Δ in a coupled channel calculation or in other ways which enhance its contribution leads to an increased $M1$ contribution and to a much better fit to the data at $E_\gamma \approx 160$ MeV. The γ asymmetry, Σ, for $E_\gamma = 30$, 60, 100, and 140 MeV are presented in Figs. 10–13. The experimental data points are the same as Ref. 6. The agreement between theory and experiment is good at $E_\gamma = 30$ and 60 MeV, but at 100 and 140 MeV it becomes poor. The much improved agreement found by Leidemann and Arenhövel[46] (see also Ref. 45) suggests that the presently used theory remains inadequate in this energy region. The work of Ref. 45 with a different treatment of the Δ in the photodisintegration leads to a considerably enhanced $M1$ matrix element for energies $E_\gamma \gtrsim 100$ MeV. Thus, it appears that even below the pion production threshold, their N-Δ coupling treatment enhances the $M1$ contribution over our work. In Figs. 9 and 13 we show the improved angular distribution and gamma asymmetry obtained if our $M1$ matrix element at 140 MeV is multiplied by an arbitrary factor of 2. The forward differential cross section is hardly affected, but, particularly the gamma-

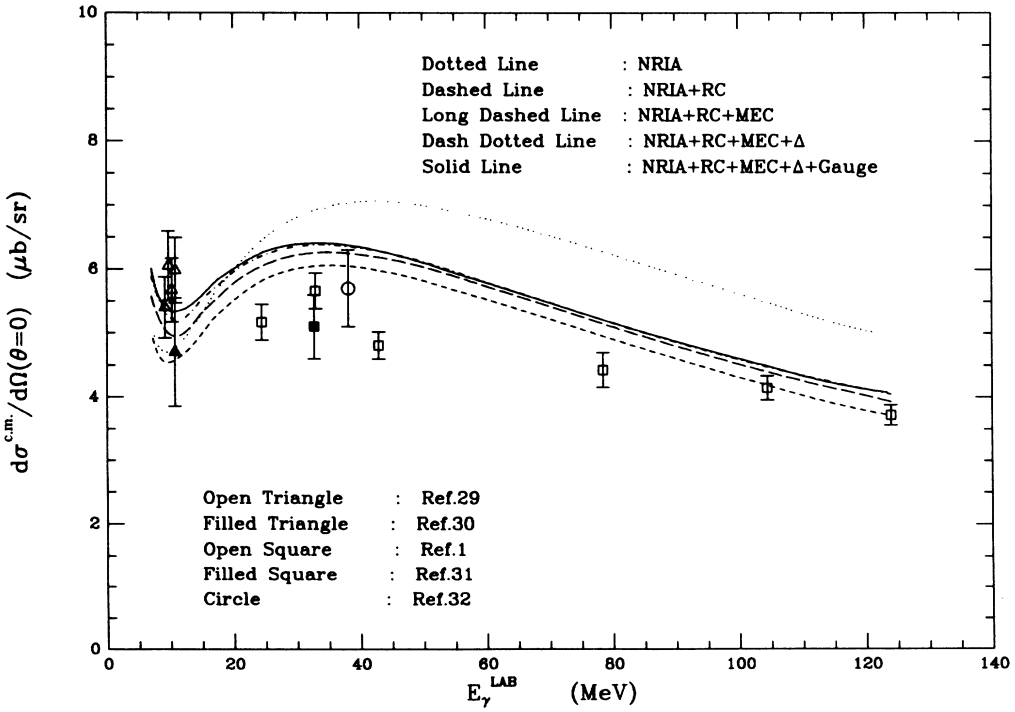

FIG. 5. Showing various corrections included in this calculation, the dotted line is NRIA, the dashed line is NRIA + RC, the long dashed line is NRIA + RC + MEC, the dash dotted line is NRIA + RC + MEC + Δ, and the solid line is NRIA + RC + MEC + Δ + gauge. The experimental points come from same source as Fig. 3.

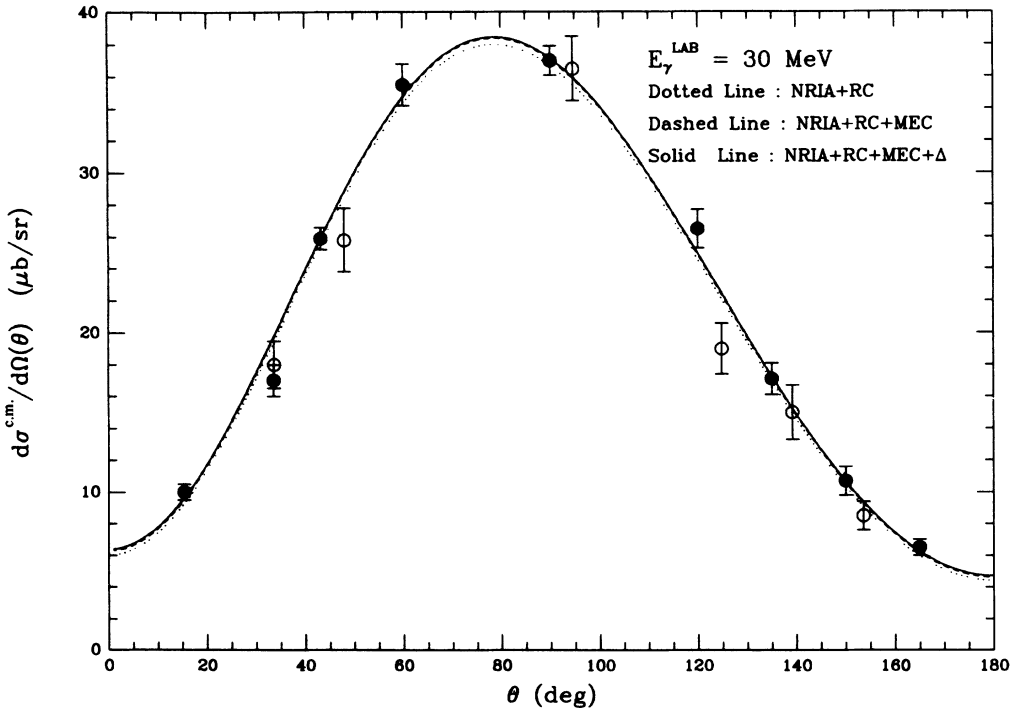

FIG. 6. Differential cross section at 30 MeV. The dotted line is NRIA + RC, the dashed line is NRIA + RC + MEC, and the solid line is NRIA + RC + MEC + Δ. Filled points are from Ref. 34 and open points are from Ref. 35 converted to the absolute value by using the total cross section given in Ref. 36.

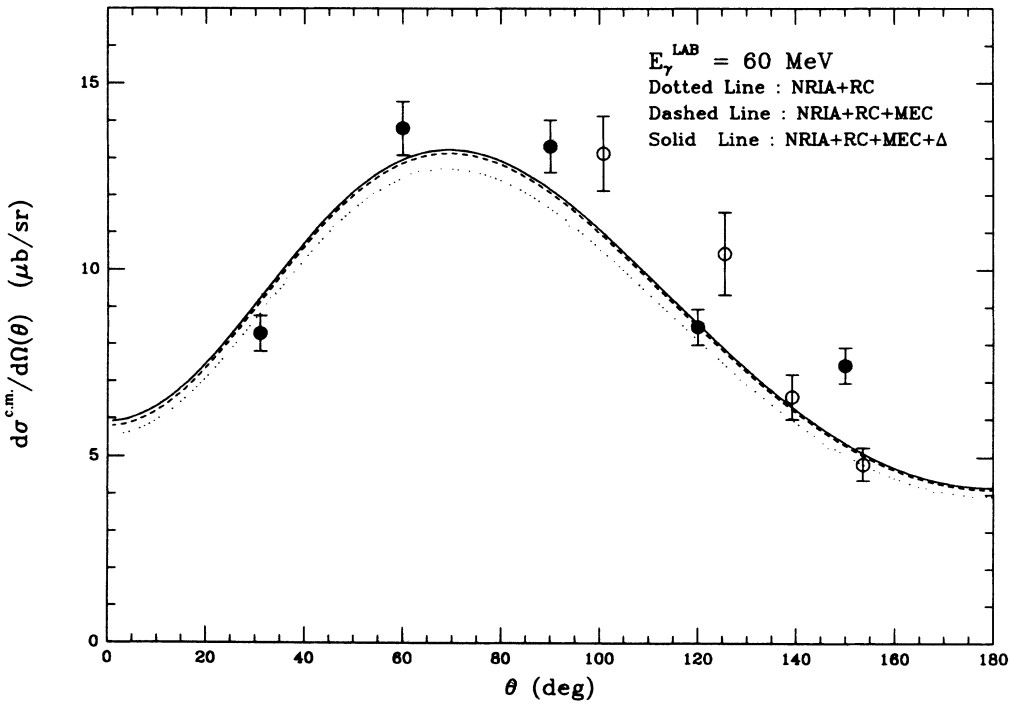

FIG. 7. Differential cross section at 60 MeV. The dotted line is NRIA + RC, the dashed line is NRIA + RC + MEC, and the solid line is NRIA + RC + MEC + Δ. Filled points are from Ref. 34 and open points are from Ref. 35 converted to the absolute value by using the total cross section given in Ref. 36.

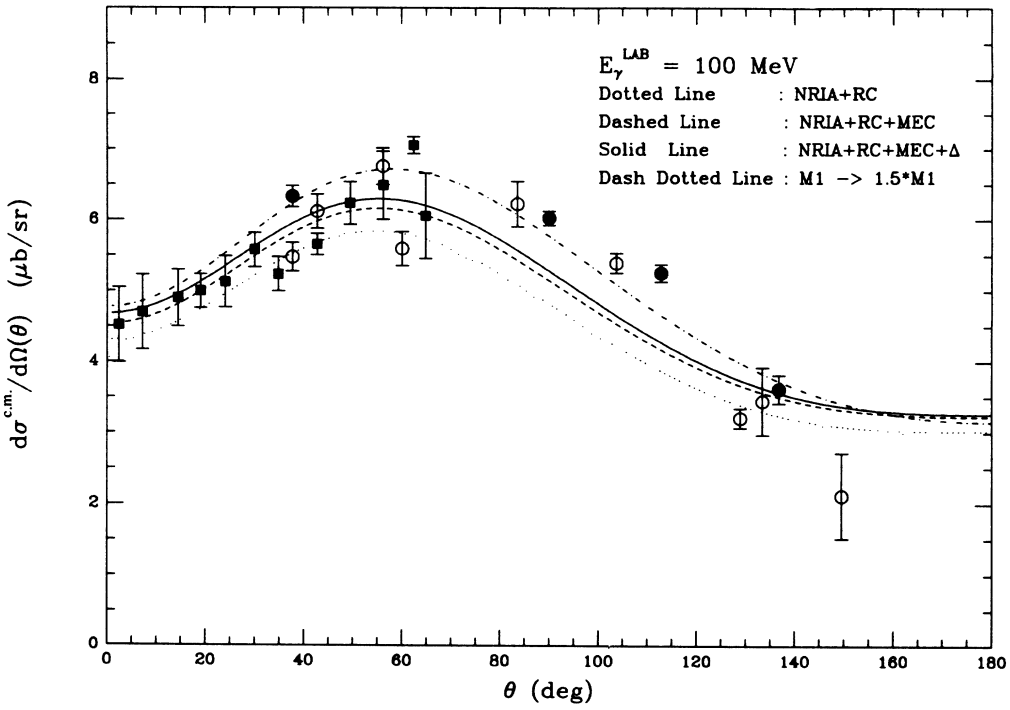

FIG. 8. Differential cross section at 100 MeV. The dotted line is NRIA + RC, the dashed line is NRIA + RC + MEC, and the solid line is NRIA + RC + MEC + Δ. The filled circle points are from Ref. 37, filled square points are from Ref. 38, and open circle points are from Ref. 39. The dash-dotted curve is obtained by multiplying the $M1$ contribution by a factor of 1.5.

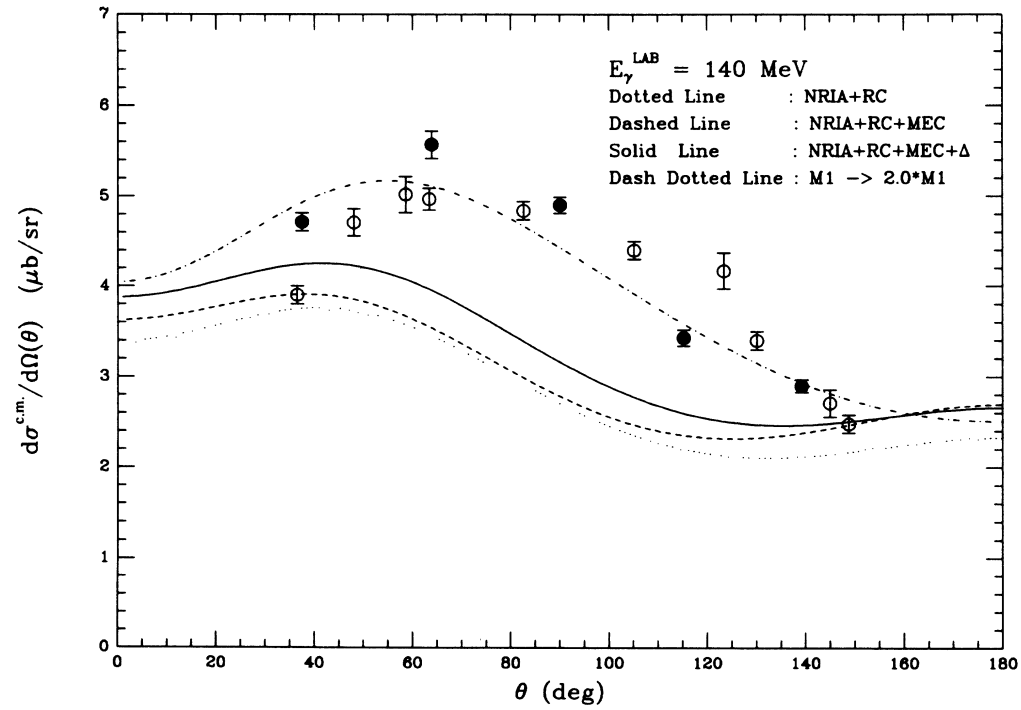

FIG. 9. Differential cross section at 140 MeV. The dotted line is NRIA + RC, the dashed line is NRIA + RC + MEC, and the solid line is NRIA + RC + MEC + Δ. The filled circle points are from Ref. 37 and the open circle points are from Ref. 39. The dash-dotted curve is obtained by multiplying the $M1$ contribution by a factor of 2.

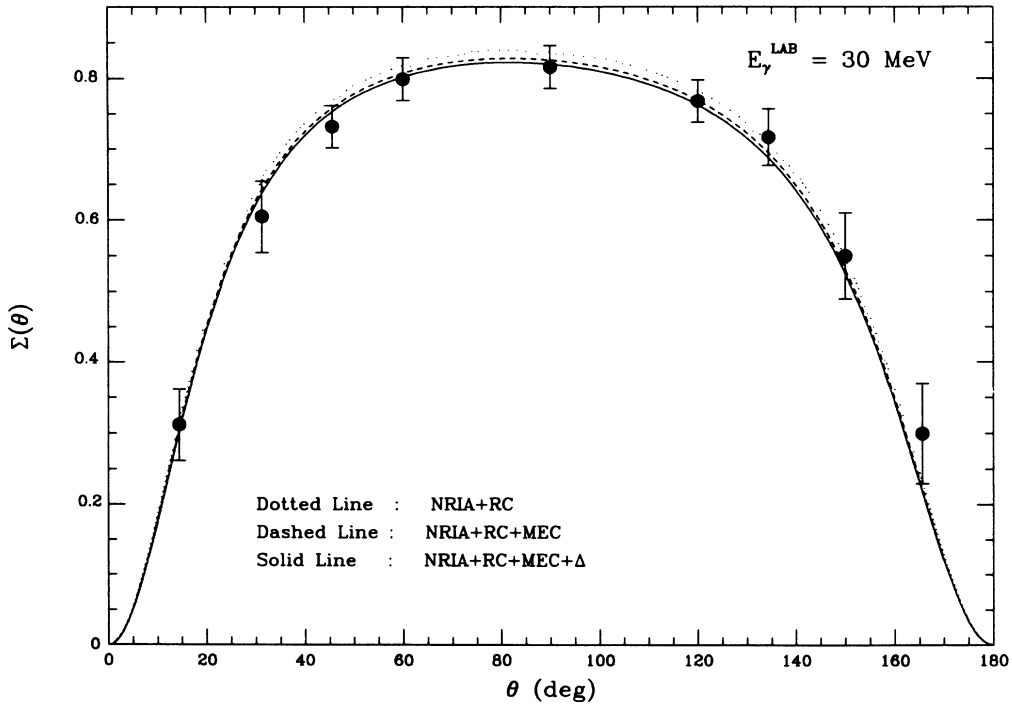

FIG. 10. γ asymmetry at 30 MeV. The dotted line is NRIA + RC, the dashed line is NRIA + RC + MEC, and the solid line is NRIA + RC + MEC + Δ. Filled circle points are from Ref. 34.

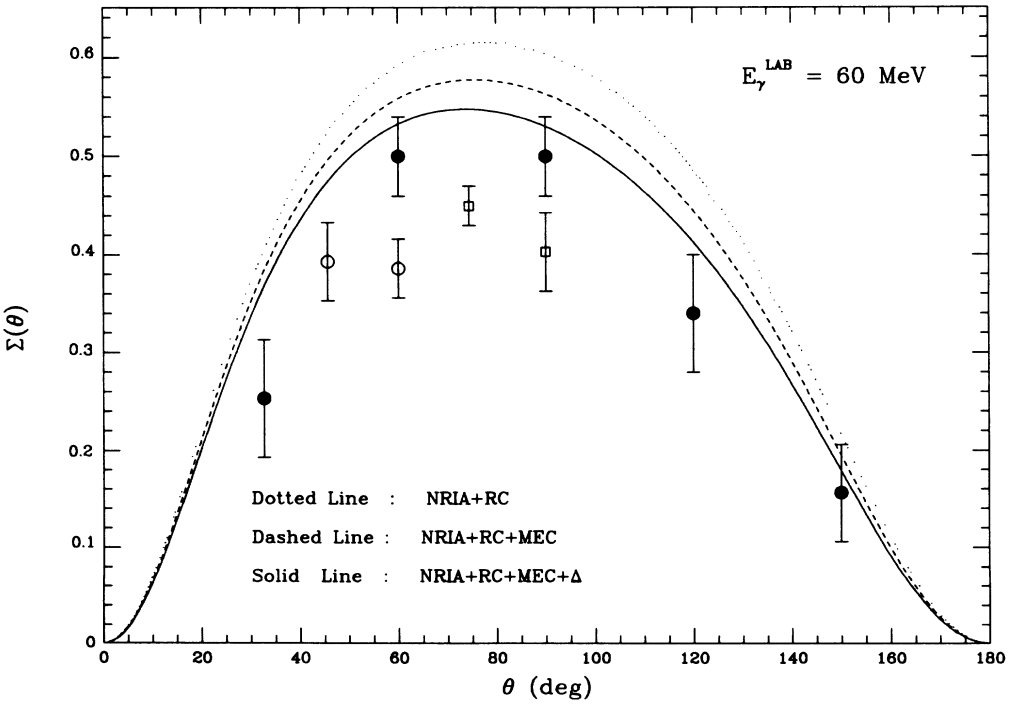

FIG. 11. γ asymmetry at 60 MeV. The dotted line is NRIA + RC, the dashed line is NRIA + RC + MEC, and the solid line is NRIA + RC + MEC + Δ. Filled circle points are from Ref. 34, open circle points are from Ref. 40, and open square points are from Ref. 41.

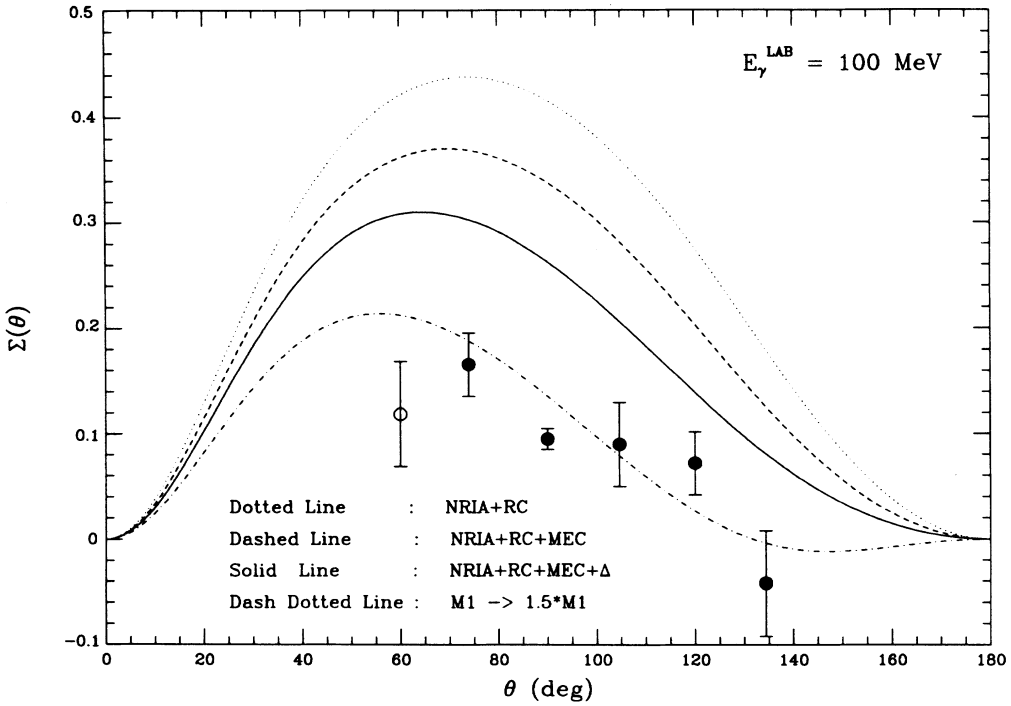

FIG. 12. γ asymmetry at 100 MeV. The dotted line is NRIA + RC, the dashed line is NRIA + RC + MEC, and the solid line is NRIA + RC + MEC + Δ. Open circle points are from Ref. 40 and filled circle points are from Ref. 42. The dash-dotted curve is obtained by multiplying the $M1$ contribution by a factor of 1.5.

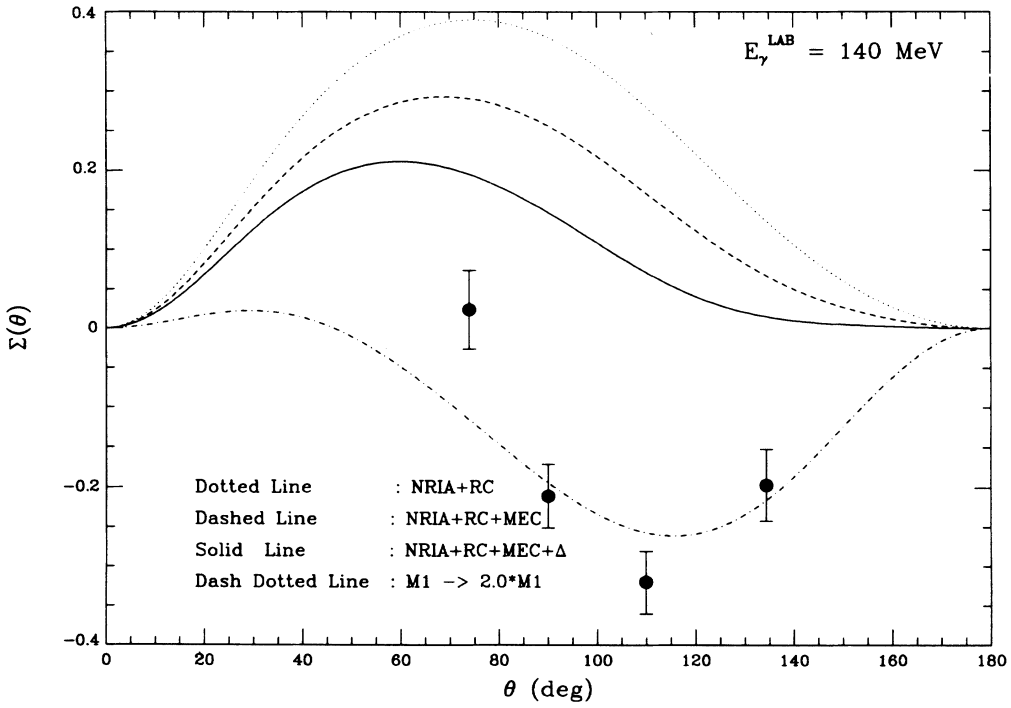

FIG. 13. γ asymmetry at 140 MeV. The dotted line is NRIA + RC, the dashed line is NRIA + RC + MEC, and the solid line is NRIA + RC + MEC + Δ. Filled circle points are from Ref. 42. The dash-dotted curve is obtained by multiplying the $M1$ contribution by a factor of 2.

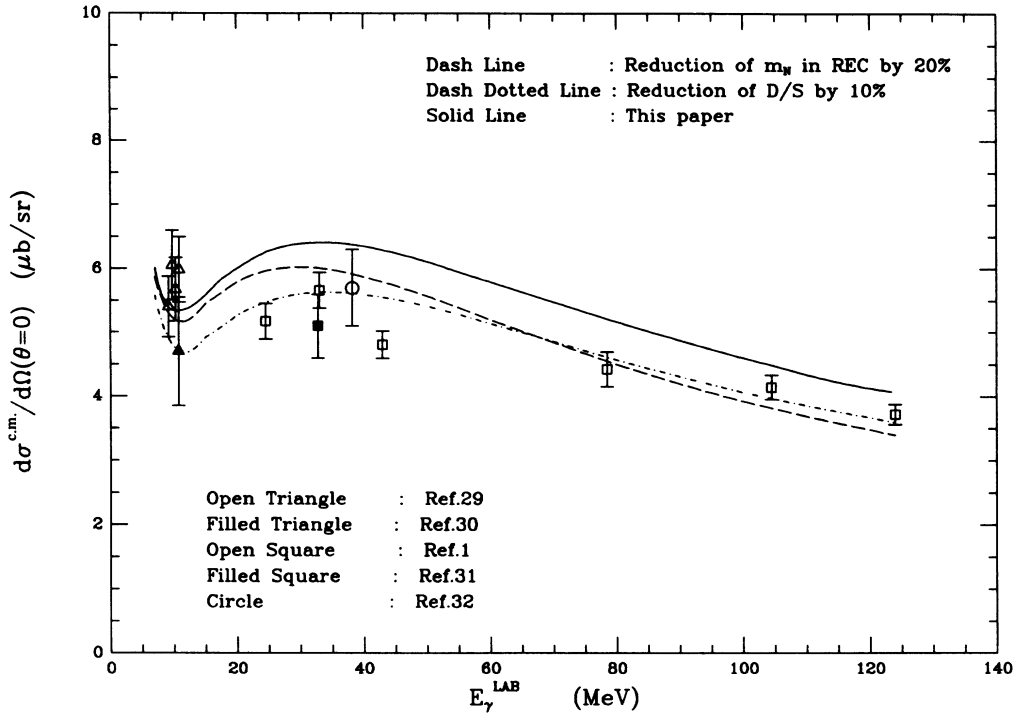

FIG. 14. Forward differential cross section. The dashed line is obtained by reducing the nucleon mass by 20% in REC; the dash-dotted line is obtained by reducing the D/S ratio by 10%; the solid line is the result of this paper without any adjustments.

ray asymmetry is altered drastically by this change. However, even Leidemann and Arenhövel do not obtain a good fit to the forward differential cross section as a function of energy.

There are some other possible explanations of the disagreements with experiment obtained in this work. First of all, it must be remembered that the sensitivity to the percentage D state is based on a fixed asymptotic D/S state ratio. If this ratio is lowered, there is a concomitant decrease in the forward differential photodisintegration differential cross section. We have investigated the sensitivity to the asymptotic D/S ratio. In Fig. 14 we show that the forward differential cross section agrees perfectly with experiment, if the asymptotic D/S ratio is lowered by 10% in the following way:

$$u \rightarrow (1+P_D\epsilon)u, w \rightarrow (1-\epsilon)w, \epsilon = 0.1$$

from the value predicted by the OBEPR Bonn potential (0.0260) and measured by Ref. 47, namely 0.0271 ± 0.0008. We have also examined the effect on the angular distribution and asymmetry of the reduction. In both cases, the disagreement is made worse; the differential cross section's shape is unchanged, so that the magnitude is smaller, whereas the asymmetry is even larger with the change. Of course it is inappropriate to simply change the D/S ratio without making other related changes. We urge our experimental colleagues to redetermine this ratio as accurately as possible, since the theoretical disagreement with experiment is clearly very sensitive to this ratio.

Another possible source of the discrepancy between theory and experiment is the electromagnetic spin-orbit interaction, which enters in the relativistic correction, Eq. (2.12a). We have also investigated the effect of changing the spin-orbit term, and find that a 20% reduction of m_N in the spin-orbit transition operator leads to agreement with the forward differential cross section, as shown in Fig. 14. In order to further investigate the effect of this change, which may also be suggested by relativistic calculations of NN scattering,[48] we have reexamined the angular distribution and asymmetry at 140 MeV, and find, again, that the agreement is made worse in that the theoretical asymmetry becomes even larger. Of course, as with the D/S ratio, it is necessary to readjust other parameters in order to make certain that the fit of the deuteron's static properties and of the N-N phase shifts is not spoiled. It is interesting that in a report just received[46] Wilhelm, Leidemann, and Arenhövel examine the effect of the same spin-orbit interaction. They also note the importance of the two-body spin-orbit effect. As already mentioned, they obtain better agreement with the experimental angular distribution and asymmetry at 160 MeV than we do at 140 MeV by treating the N and Δ as coupled channels.

In conclusion, we have examined the deuteron photodisintegration with the Bonn potential for an energy region below the delta resonance. We find an insensitivity to the deuteron D-state probability as long as the asymptotic D/S ratio is kept fixed. The forward differential cross section is very sensitive to this asymptotic ratio as well as to the spin-order force. Our forward differential cross section remains somewhat high relative to experiment. To fit the angular distribution and γ-asymmetry above ~ 100 MeV, it appears that a calculation which improves the treatment of the Δ and enhances the $M1$ contribution is required.

ACKNOWLEDGMENTS

We wish to thank Mr. Douglas Driscoll for providing computing assistance, and Prof. H. Arenhövel for informing us of his work prior to publication. This work is supported in part by the U.S. Department of Energy.

APPENDIX A: MATRIX ELEMENTS FOR EXTENDED SIEGERT THEOREM

Define the radial integral $I_{l_i s_i J_i}^{l_f s_f J_f}[F]$ as

$$I_{l_i s_i J_i}^{l_f s_f J_f}[F]=\frac{1}{k}\int_0^\infty dr\, u_{l_f s_f J_f}(kr)F(r)v_{l_i s_i J_i}(r) \tag{A1}$$

and the reduced matrix element as

$$\langle J_f m_f \mid O_{J_m} \mid J_i m_i\rangle=(-1)^{J_i-J-m_f}\begin{bmatrix} J_i & J & J_f \\ m_i & m & -m_f\end{bmatrix}\langle J_f\|O_J\|J_i\rangle\ , \tag{A2}$$

where k is the relative momentum of the p and n and F is a function of r. The reduced matrix of $T_{Jm}^{\rm el}$ is

$$\begin{aligned}
&\langle J_f(l_f s_f)\|T_J^{\rm el}\|J_i(l_i s_i)\rangle \\
&=\frac{q^{J-1}}{(2J+1)!!}\left\{-q\left[\frac{J+1}{J}\right]^{1/2} I_{l_i s_i J_i}^{l_f s_f J_f}\left[\left[\frac{r}{2}\right]^J g_J(\tfrac{1}{2}qr)\right]\langle J_f(l_f s_f)\|Y_J\|J_i(l_i s_i)\rangle\right. \\
&\quad+\frac{q^2}{4M}\frac{[J(J+1)]^{1/2}}{J+2} I_{l_i s_i J_i}^{l_f s_f J_f}\left[\left[\frac{r}{2}\right]^J h_J(\tfrac{1}{2}qr)\right]\langle J_f(l_f s_f)\|Y_J\|J_i(l_i s_i)\rangle \\
&\quad+\frac{q^2}{2M}\frac{1}{J+2} I_{l_i s_i J_i}^{l_f s_f J_f}\left[\left[\frac{r}{2}\right]^J h_J(\tfrac{1}{2}qr)\right]\langle J_f(l_f s_f)\|[Y_J\otimes L]^J\|J_i(l_i s_i)\rangle \\
&\quad\left.+\frac{q^2\mu^{s/v}}{2M}\frac{1}{J+2} I_{l_i s_i J_i}^{l_f s_f J_f}\left[r\frac{d}{dr}\left[\frac{r}{2}\right]^J h_J(\tfrac{1}{2}qr)2\left[\frac{r}{2}\right]^J h_J(\tfrac{1}{2}qr)\right]\langle J_f(l_i s_i)\|[Y_J\otimes\Sigma]^J\|J_i(l_i s_i)\rangle\right\}\ ,
\end{aligned} \tag{A3}$$

where $\mu^{s/v}=\mu^s$ or μ^v depend on the isospin transition,

$$\langle J_f(l_f s_f)\|Y_J\|J_i(l_i s_i)\rangle i^J=(-1)^{l_f+s_i+J_i+J}\tilde{J}_i\tilde{J}_f\langle l_f\|Y_J\|l_i\rangle\begin{Bmatrix} l_f & J_f & s_i \\ J_f & l_i & J\end{Bmatrix}\ ,$$

$$\langle J_f(l_f s_f)\|[Y_K\otimes L]^J\|J_i(l_i s_i)\rangle i^K=(-1)^{l_i+s_i+J_i}\tilde{J}_i\tilde{J}_f\tilde{J}\langle l_f\|Y_K\|l_i\rangle\langle l_i\|L\|l_i\rangle\begin{Bmatrix} l_f & J_f & s_i \\ J_i & l_i & J\end{Bmatrix}\begin{Bmatrix} K & 1 & J \\ l_i & l_f & l_i\end{Bmatrix}\ ,$$

$$\langle J_f(l_i s_i)\|[Y_K\otimes\Sigma]^J\|J_i(l_i s_i)\rangle i^K=\tilde{J}_i\tilde{J}_f\tilde{J}\langle l_f\|Y_K\|l_i\rangle\langle s_f\|\Sigma\|s_i\rangle\begin{Bmatrix} l_f & l_i & K \\ s_f & s_i & 1 \\ J_f & J_i & J\end{Bmatrix}\ ,$$

L is the angular momentum operator, $\Sigma=(S_1\pm S_2)$ and $\tilde{L}=\sqrt{2L+1}$. We use the phase convention of Partovi, including the i^l factor in front of Y_{lm} and the sign difference between ϵ^j and the BB convention.[33] The relationship between $T_{Jm}^{\rm el}$ and the matrix element defined by Eq. (52) in Ref. 2 for the deuteron is

$$\langle sm_s \mid E^L \mid m_d\rangle=\sum_{\lambda J_f l_f s_f}[4\pi(2l_f+1)]^{1/2}\langle l_f 0 s_f m_s \mid J_f m_s\rangle e^{i\delta_\lambda^{J_f}} U_{l_f s_f\lambda}^{J_f}\langle 1m_d;Jm \mid J_f ms\rangle\langle J_f\lambda\|\tilde{T}_J^{\rm el}\|1\rangle\ , \tag{A4}$$

$$\langle J_f\lambda\|\tilde{T}_J^{\rm el}\|1\rangle=\left[\frac{\alpha k m_N(2J+1)}{2q}\right]^{1/2}\sum_{l_f l_i} U_{l_f s_f\lambda}^{J_f}\langle J_f(l_f s_f)\|T_J^{\rm el}\|1(l_i 1)\rangle\ , \tag{A5}$$

where α is the fine structure constant, m_N is the nucleon mass, and q the photon energy, and $\langle l_1 m_1;l_2 m_2 \mid Jm\rangle$ is the Clebsch-Gordan coefficient. The magnetic part of the matrix element is the same for all gauges. It can be found elsewhere.

APPENDIX B: THE CONTRIBUTION OF CURRENT GENERATED FROM THE NONLOCAL PART OF THE POTENTIAL

We follow the convention in Appendix A. The reduced matrix elements are

$$\langle J_f(l_f s_f)\|T_J^{\rm el}\|J_i(l_i s_i)\rangle = -\frac{q^{J+1}}{\sqrt{2}(J+2)(2J+1)!!}\{i^J\langle J_f(l_f s_f)\|[Y_J\otimes L]^J\|J_i(l_i s_i)\rangle I_1^{(e)} + 2i^J\langle J_f(l_f s_f)\|[Y_J\otimes S]^J\|J_i(l_i s_i)\rangle I_2^{(e)}\}\ , \tag{B1}$$

$$\langle J_f(l_f s_f)\|T_J^{\rm mag}\|J_i(l_i s_i)\rangle = (-i)^J\sqrt{4\pi}\left[\left[\sum_{K=J\pm1}\tilde{K}\langle K\|Y_J\|1\rangle\begin{Bmatrix} J & 1 & J\\ 1 & K & 1\end{Bmatrix} i^K\langle J_f(l_f s_f)\|[Y_K\otimes L]^J\|J_i(l_i s_i)\rangle\right] I_1^m + \left[\sum_{K=J\pm1}\tilde{K}\langle K\|Y_J\|1\rangle\begin{Bmatrix} J & 1 & J\\ 1 & K & 1\end{Bmatrix} i^K\langle J_f\|[Y_K\otimes S]^J\|J_i\rangle\right] I_2^m\right]\ , \tag{B2}$$

where

$$\langle J_f(l_f s_f)\|Y_J\|J_i(l_i s_i)\rangle\ ,$$

$$\langle J_f(l_f s_f)\|[Y_K\otimes L]^J\|J_i(l_i s_i)\rangle\ ,$$

$$\langle J_f\|[Y_K\otimes S]^J\|J_i\rangle\ ,$$

and are given in Appendix A. Also, we have

$$I_1^e = \frac{1}{k}\int_0^\infty dr\, u_{J_f l_f s_f}(kr)\tilde{O}(r)\left[\frac{r}{2}\right]^J h_J(\tfrac{1}{2}qr)v_{J_i l_i s_i}(r)\ , \tag{B3}$$

$$I_2^e = \frac{1}{k}\int_0^\infty dr\, u_{J_f l_f s_f}(kr)\tilde{O}^{\,LS}(r)\left[\frac{r}{2}\right]^{J+2} h_J(\tfrac{1}{2}qr)v_{J_i l_i s_i}(r)\ , \tag{B4}$$

$$I_1^m = \frac{1}{k}\int_0^\infty dr u_{J_f l_f s_f}(kr)\tilde{O}(r)j_J(\tfrac{1}{2}qr)v_{J_i l_i s_i}(r)\ , \tag{B5}$$

$$I_2^m = \frac{1}{k}\int_0^\infty r^2 d\, r u_{J_f l_f s_f}(kr)\tilde{O}^{\,LS}(r)j_J(\tfrac{1}{2}qr)v_{J_i l_i s_i}(r)\ , \tag{B6}$$

and the operators O and O^{LS} are related to the nonlocal part of the potential by

$$V_{\rm nonlocal} = \nabla^2\tilde{O}(r) + \tilde{O}\nabla^2 + \tilde{O}^{\,LS}(r)\mathbf{L}\cdot\mathbf{S}\ .$$

[1] R. J. Hughes, A. Zieger, H. Waffler, and B. Ziegler, Nucl. Phys. **A267**, 329 (1976).
[2] F. Partovi, Ann. Phys. (N.Y.) **27**, 79 (1962).
[3] H. Arenhövel and W. Fabian, Nucl. Phys. **A282**, 397 (1977).
[4] E. L. Lomon, Phys. Lett. **68B**, 419 (1977).
[5] L. Rustgi, T. S. Sandhu, and O. P. Rustgi, Phys. Lett. **70B**, 145 (1977); Nucl. Phys. C **20**, 24 (1979).
[6] W. Jaus and W. S. Woolcock, Nucl. Phys. **A473**, 667 (1987).
[7] M. Lacombe, B. Loiseau, J. M. Richard, R. Vinh mau, J. Côté, P. Pirés, and R. de Tourreil, Phys. Rev. C **21**, 861 (1980).
[8] R. Machleidt, K. Holinde, and Ch. Elster, Phys. Rep. **149**, 1 (1987).
[9] A. Cambi, B. Mosconi, and P. Ricci, Phys. Rev. Lett. **48**, 462 (1982).
[10] K. W. McVoy and L. Van Hove, Phys. Rev. **125**, 1034 (1962); T. De Forest, Jr. and J. D. Walecka, Adv. Phys. **15**, 1 (1966).
[11] W. Jaus and W. S. Woolcock, Helv. Phys. Acta. **57**, 644 (1984).
[12] R. Blankenbecler and R. Sugar, Phys. Rev. **142**, 1051 (1966).
[13] See, e.g., J. L. Friar, Nucl. Phys. **A264**, 455 (1976); F. Coester and P. Havas, Phys. Rev. D **14**, 2556 (1976).
[14] J. L. Friar, Phys. Rev. C **22**, 796 (1980); H. Hyuga and M. Gari, Nucl. Phys. **A274**, 333 (1976).
[15] H. Arenhövel and W. Fabian, in *Few Body System and Electromagnetic Interaction,* edited by J. Ehlers, in *Lecture Notes in Physics* (Springer-Verlag, Berlin, 1978), p. 85–100.
[16] F. J. Dyson, Phys. Rev. **73**, 929 (1948).
[17] J. L. Friar, Ann. Phys. (N.Y.) **104**, 380 (1977).
[18] J. L. Friar, B. F. Gibson, and G. L. Payne, Phys. Rev. C **30**, 441 (1984).
[19] R. K. Osborn and L. L. Foldy, Phys. Rev. **79**, 795 (1950).
[20] F. Partovi, Phys. Rev. C **36**, 491 (1987).
[21] A. J. F. Siegert, Phys. Rev. **52**, 787 (1937).
[22] L. L. Foldy, Phys. Rev. **92**, 178 (1953).
[23] J. L. Friar and S. Fallieros, Phys. Rev. C **29**, 1645 (1984).
[24] W.-Y.P. Hwang, Phys. Rev. C **21**, 1086 (1980).

[25]T. Hamada and I. D. Johnston, Nucl. Phys. **34**, 382 (1962).
[26]W. Jaus and W. S. Woolcock, Nucl. PHys. **A431**, 669 (1984).
[27]H. T. Williams, Phys. Rev. C **31**, 2297 (1985).
[28]R. E. Behrends and C. Fronsdal, Phys. Rev. **106**, 345 (1957).
[29]A. De Graeve *et al.*, Interim report of the Nuclear Physics Laboratory—Gent State University, Gent, Belgium, 1986.
[30]A. Zieger, P. Grewer, and B. Zieger, Few-Body Syst. **1**, 135 (1986).
[31]A. Ninane, C. Dupont, P. Leleux, P. Lipnik, and P. Macq, Can. J. Phys. **62**, 1104 (1984).
[32]J. F. Gilot, A. Bol, P. Leleux, P. Lipnik, and P. Macq, Phys. Rev. Lett. **47**, 304 (1981).
[33]J. M. Blatt and L. C. Biedenharn, Phys. Rev. **86**, 399 (1952).
[34]M. P. De Pascale *et al.*, Phys. Rev. C **32**, 1830 (1985).
[35]B. Weissman and H. L. Schultz, Nucl. Phys. **A174**, 129 (1971).
[36]R. Bernabei *et al.*, Phys. Rev. Lett. **57**, 1542 (1986).
[37]E. De Sanctis *et al.*, Phys. Rev. Lett. **54**, 1639 (1985).
[38]H. O. Meyer, J. R. Hall, M. Hugi, H. J. Karwowski, R. E. Pollock, and R. Schwandt, Phys. Rev. C **31**, 309 (1985).
[39]J. M. Cameron *et al.*, Nucl. Phys. **A458**, 637 (1986).
[40]I. E. Vnukov *et al.*, Pis'ma Zh. Eksp. Teor. Fiz. **43**, 510 (1986) [Sov. Phys.—JETP Lett. **43**, 659 (1986)].
[41]V. P. Barannik *et al.*, Sov. J. Nucl. Phys. **38**, 667 (1983).
[42]V. G. Gorbenko *et al.*, Sov. J. Nucl. Phys. **35**, 627 (1982).
[43]J. L. Friar and W. C. Haxton, Phys. Rev. C **31**, 2027 (1985).
[44]J. L. Friar and S. Fallieros, Phys. Rev. C **34**, 2029 (1986).
[45]W. Leidemann and H. Arenhövel, Nucl. Phys. **A465**, 573 (1987).
[46]P. Wilhelm, W. Leidemann, and H. Arenhövel (unpublished).
[47]N. L. Rodning and L. D. Knutson, Phys. Rev. Lett. **57**, 2248 (1986).
[48]S. J. Wallace, Ann. Rev. Nucl. Part. Sci. **37**, 267 (1987).